

Efficient Transient Full-Wave Analysis of High-Speed Interconnects in Multilayer PCBs

Ali Akbarzadeh-Sharbat and Dennis D. Giannacopoulos

Department of Electrical and Computer Engineering, McGill University, Montréal, Québec H3A 0E9, Canada

Email: ali.sharbat@mail.mcgill.ca, dennis.giannacopoulos@mcgill.ca

Abstract—A new approach to efficiently simulate 3-D high-speed multilayer printed circuit boards (PCBs) using the finite-element time-domain (FETD) method is proposed. The method is based on the discretization of these structures using multiple layers of prism finite elements. In order to eliminate coupling between different layers in the mass matrix, a combined exact/approximate numerical integration technique is applied to the finite element matrices. This makes the final mass matrix fully block-diagonal and greatly reduces the inversion/factorization cost and time. The formulation is readily extended to lossy materials without any additional adverse effect on the stability condition.

Index Terms—Finite-element methods, interconnect, printed circuit board (PCB), transient analysis.

I. INTRODUCTION

There is an emerging need for developing innovative full-wave electromagnetic simulation algorithms enabling researchers to efficiently model (ultra-)large-scale problems. Multilayer structures are an important class of systems that can embrace a large range of devices widely in use, such as high-frequency multilayer PCBs, interconnects, and integrated circuits (ICs). This geometric property, i.e., layeredness, significantly simplifies the mesh generation: details of all layers are first projected onto a surface and meshed by a 2-D mesher, then the 3-D mesh can be obtained by extruding the 2-D one along the layer-growth direction. As shown in Fig. 1 for a simple coaxial cable, the final mesh consists of several stacked layers of prism mesh. This approach was employed to reduce mesh generation cost in antenna [1], deep cavity [2], and multilayer circuit [3] problems. Jiao made use of this property to speedup the finite-element simulation of ICs in both the frequency and time domain [4], [5]. The algorithm that she proposed involves *reducing* the mass matrix into that of a single layer, and then *recovering* the solution of the original problem from that of the reduced problem. The proposed approach involves multiple *reduction* and *recovery* steps. Moreover, the stability condition of the FETD formulation is severely tightened in the presence of the lossy materials. For example, it is three orders of magnitude smaller than the conventional stability condition in a typical on-chip problem discussed in [6]. They proposed an iterative algorithm to alleviate this problem [6], which has a problem-dependent convergence rate.

In this work, a new approach to reduce the computational cost associated with the FETD simulation of layered structures discretized using prism elements is introduced. The method

decouples transverse triangular grids from each other to yield a fully block-diagonal mass matrix. This is achieved by using a combination of exact and numerical integrations to evaluate the mass matrix. The number of blocks is equal to $2N + 1$ for an N -layer problem. Hence, a tremendous saving in time and, particularly, memory required to directly solve the system of equations is achieved, which is the principal challenge in full-wave simulations. The method does not involve reduction/recovery steps and can simply model lossy materials without imposing any additional restriction on the stability condition. The method can be considered as a *mass-lumping* method for prism finite elements along the longitudinal direction.

II. FORMULATION

The FETD solution can be obtained by solving the following system of the ordinary differential equations (ODE)

$$\varepsilon[\mathcal{M}] \frac{\partial^2 \{e\}}{\partial t^2} + \sigma[\mathcal{R}] \frac{\partial \{e\}}{\partial t} + \mu^{-1}[\mathcal{S}]\{e\} = \{f\} \quad (1)$$

in which the impressed current source is injected through the vector $\{f\}$ and the matrices are defined as

$$\mathcal{M}_{i,j} = \mathcal{R}_{i,j} = \int_{\Omega} \mathbf{N}_i \cdot \mathbf{N}_j dV \quad (2)$$

$$\mathcal{S}_{i,j} = \int_{\Omega} \nabla \times \mathbf{N}_i \cdot \nabla \times \mathbf{N}_j dV. \quad (3)$$

Discretizing (1) using the central-difference method gives the following system of equations

$$\begin{aligned} \left\{ \varepsilon[\mathcal{M}] + \frac{\sigma \Delta t}{2} [\mathcal{R}] \right\} \{e\}^{n+1} &= \left\{ 2\varepsilon[\mathcal{M}] - \frac{(\Delta t)^2}{\mu} [\mathcal{S}] \right\} \{e\}^n \\ &- \left\{ \varepsilon[\mathcal{M}] - \frac{\sigma \Delta t}{2} [\mathcal{R}] \right\} \{e\}^{n-1} + (\Delta t)^2 \{f\}^n. \end{aligned} \quad (4)$$

Fig. 2 shows a prism finite element with the height of h along the ζ -axis in which the vector basis functions are

$$\begin{aligned} \mathbf{N}_1 &= \frac{\zeta}{h} (\xi_1 \nabla \xi_2 - \xi_2 \nabla \xi_1) = \frac{\zeta}{h} \mathbf{W}_1 \\ \mathbf{N}_2 &= \frac{\zeta}{h} (\xi_1 \nabla \xi_3 - \xi_3 \nabla \xi_1) = \frac{\zeta}{h} \mathbf{W}_2 \\ \mathbf{N}_3 &= \frac{\zeta}{h} (\xi_2 \nabla \xi_3 - \xi_3 \nabla \xi_2) = \frac{\zeta}{h} \mathbf{W}_3 \\ \mathbf{N}_4 &= \xi_1 \hat{\zeta}, \mathbf{N}_5 = \xi_2 \hat{\zeta}, \mathbf{N}_6 = \xi_3 \hat{\zeta} \\ \mathbf{N}_7 &= \frac{h-\zeta}{h} \mathbf{W}_1, \mathbf{N}_8 = \frac{h-\zeta}{h} \mathbf{W}_2, \mathbf{N}_9 = \frac{h-\zeta}{h} \mathbf{W}_3 \end{aligned}$$

where ξ and \mathbf{W} represent the nodal and edge basis functions of a triangle.

In order to calculate the integrals in (2)-(3), the volume integral element can be expressed as: $dV = dAd\zeta$ in which dA denotes the surface integral element in the transverse cross section perpendicular to ζ . Due to the orthogonality, the longitudinal unknowns (vertical edges) are already decoupled from transverse (horizontal) ones in the $[\mathcal{M}]$ matrix; however, all transverse unknowns residing in different layers are still coupled to each other, if the integral is evaluated exactly. Alternatively, we can only evaluate the surface integral exactly and employ an appropriate numerical integration technique for $d\zeta$. Since the order of ζ does not exceed one in the basis functions, the trapezoidal rule is a valid choice [7], which involves

$$\int_a^b f(x) \simeq \frac{b-a}{2} (f(a) + f(b)). \quad (5)$$

For a single layer of the prism grid, which can be arbitrarily extended along other directions rather than ζ , applying the above approach to the mass matrix gives the following block-diagonal matrix

$$[\mathcal{M}] = \begin{bmatrix} [M_L] & 0 & 0 \\ 0 & [M_\zeta] & 0 \\ 0 & 0 & [M_U] \end{bmatrix}$$

in which $[M_L]$, $[M_U]$, and $[M_\zeta]$ represent the interaction among lower triangular surface edges, upper triangular surface edges, and edges along ζ (volume edges), respectively, in which $[M_L] = [M_U]$. If the actual 3-D mesh is composed of N layers, the final mass matrix will be

$$[\mathcal{M}] = \text{diag}([M_{L_1}], [M_{\zeta_1}], [M_{U_1}] + [M_{L_2}], [M_{\zeta_2}], \dots, [M_{U_N}]). \quad (6)$$

This matrix is composed of $2N + 1$ block matrices, which greatly reduces the factorization/solve cost specially for large-scale problems. When the structure contains some identical layers, which is very likely, a further reduction in cost is possible, because they share identical blocks. For instance, if all layers are identical to each other, we only need to factorize two sub-matrices: $[M_{U_1}]$ and $[M_{\zeta_1}]$.

Unfortunately, such a sparsification is not obtained for the stiffness matrix due to the presence of the curl operator. This matrix can be evaluated exactly; however, our numerical studies showed that both approaches give quite similar results. Because, the ζ variable is eliminated by the curl operator in most of the terms.

As can be interpreted from (2), the $[\mathcal{R}]$ matrix can be block-diagonalized in exactly the same way. Hence, the left-hand side (LHS) of (4) has an identical sparsity pattern as $[\mathcal{M}]$ and lossy materials can be simply included in the simulation without adding extra cost in factorization or limiting the stability condition.

III. NUMERICAL STUDIES

As the first example, pulse propagation along a 3 cm long, air-filled coaxial cable is considered. The inner and

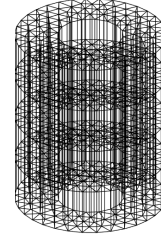


Fig. 1: A coaxial cable meshed by 4 layers of prism grids.

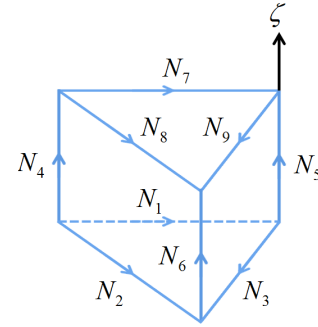


Fig. 2: A prism finite element.

outer radii of the cable are 1 mm and 2.3 mm, respectively. The cross-section of the cable is discretized by 220 triangles with the average edge length of 0.38 mm and extruded along the propagation direction to form 78 identical prismatic layers. Both sides of the cable are truncated with a first-order absorbing boundary condition (ABC), and the time-step is set to 0.3 ps. The TEM mode with a Gaussian pulse shape was launched at one side of the cable and the voltage at the other side of the cable was recorded. Fig. 3 shows the voltage obtained from simulation, which matches with the exact solution excellently. Moreover, a huge saving on the computation time is also made. Factorization of the LHS matrix calculated with exact integration took 262 ms compared to the 18.6 ms of the mass-lumped one. This saving in time will be more tangible in large-scale simulations. The required time for the time-marching process, which includes 1000 time-steps, was 18.45 s and 2.50 s for each case. Due to homogeneity of the cable, the mass matrix is composed of only three unique blocks. Making use of this property can further accelerate simulation and save much more memory, which has not been studied in this paper.

The second example is a relatively large via hole problem. Fig. 4 shows two pairs of differential vias passing through a seven layer PCB [8]. The via holes are connected together by 50 cm long striplines. The thickness of the metallization is 0.035 mm and the substrate has a relative permittivity of $\epsilon_r = 4 - j0.06$. Half of the problem is considered, due to the symmetry, to find the solution. The structure, except the coaxial ports, are divided into 65 layers of prism grids. Applying the linear basis functions yields 2,313,478 unknowns. Factorizing the mass-lumped LHS matrix took only 3.33 s with a peak memory of 1.038 GB; whereas, a PC

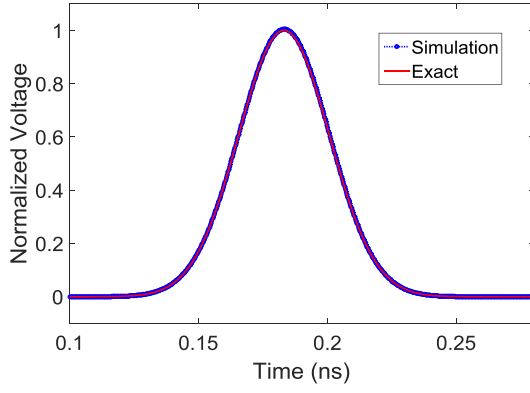


Fig. 3: Time-domain Gaussian pulse propagating through the empty coaxial cable and recorded at one side of it.

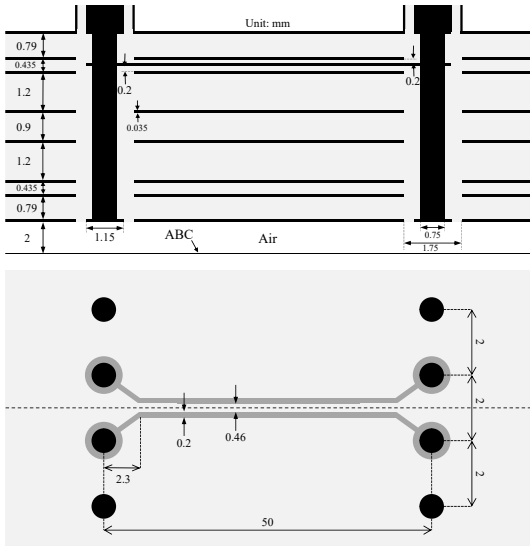


Fig. 4: Side and top views of the differential via pairs in a seven-layer PCB.

with 32 GB of memory was not able to factorize the non-mass-lumped one. Fig. 5 and Fig. 6 show the differential mode S-parameters of the problem along with the FEM and measurement results taken from [3] and [8].

IV. CONCLUSION

Evaluating the mass matrix of the prism mesh generated from a multilayer PCB using a combination of trapezoidal and exact integration has turned the mass matrix into a fully block-diagonal one consisting of $2N + 1$ blocks for an N -layer problem. This not only greatly accelerates simulation and saves computational power and memory, but also enables the researchers to simulate much larger problems on a given PC. The numerical studies have demonstrated that although a great saving in the computational cost is achieved, no significant error due to the mass-lumping has occurred. This method can be extended to high-order basis functions and dispersive materials.

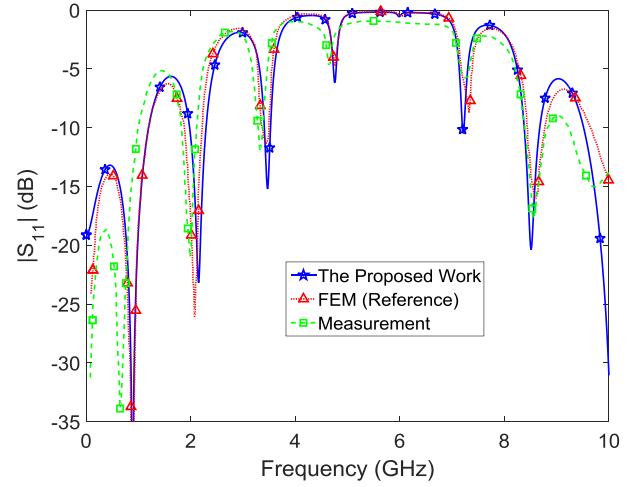


Fig. 5: $|S_{11}|$ of the differential via example.

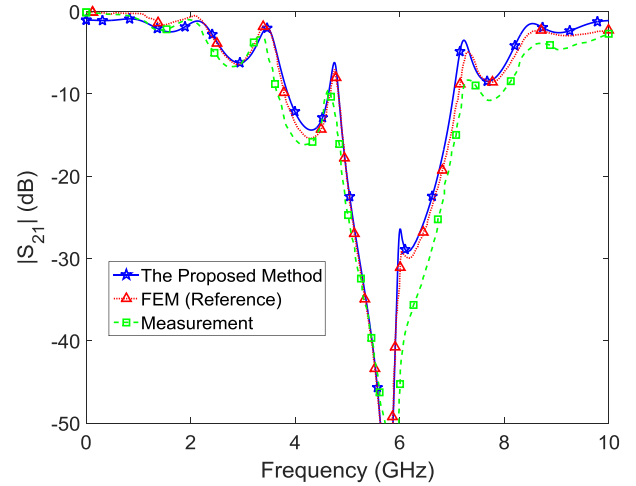


Fig. 6: $|S_{21}|$ of the differential via example.

REFERENCES

- [1] T. Özdemir and J. L. Volakis, "Triangular prisms for edge-based vector finite element analysis of conformal antennas," *IEEE Trans. Antennas Propag.*, vol. 45, no. 5, pp. 788–797, May 1997.
- [2] J. Liu and J.-M. Jin, "A special higher order finite-element method for scattering by deep cavities," *IEEE Trans. Antennas Propag.*, vol. 48, no. 5, pp. 694–450, May 2000.
- [3] K. Mao, "Finite element analysis of multilayer transmission lines and circuit components," Ph.D. dissertation, University of Illinois at Urbana-Champaign, Urbana, IL, 2007.
- [4] D. Jiao, S. Chakravarty, and C. Dai, "A layered finite element method for electromagnetic analysis of large-scale high-frequency integrated circuits," *IEEE Trans. Antennas Propag.*, vol. 55, no. 2, pp. 422–432, Feb. 2007.
- [5] H. Gan and D. Jiao, "A time-domain layered finite element reduction recovery (LAFE-RR) method for high-frequency VLSI design," *IEEE Trans. Antennas Propag.*, vol. 55, no. 12, pp. 3620–3629, Dec. 2007.
- [6] —, "A fast-marching time-domain layered finite-element reduction-recovery method for high-frequency VLSI design," *IEEE Trans. Antennas Propag.*, vol. 57, no. 2, pp. 577–581, Feb. 2009.
- [7] R. Lee, "A note on mass lumping in the finite element time domain method," *IEEE Trans. Antennas Propag.*, vol. 54, no. 2, pp. 760–762, Feb. 2006.
- [8] E. Laermans *et al.*, "Modeling complex via hole structures," *IEEE Trans. Microw. Theory Tech.*, vol. 25, no. 2, pp. 206–214, May 2002.